Acta metall. mater. Vol. 41, No. 10, pp. 2963–2971, 1993
Printed in Great Britain.

0956-7151/93 $6.00 + 0.00

INTERFACIAL REACTION WETTING IN THE BORON NITRIDE/MOLTEN ALUMINUM SYSTEM

H. FUJII, H. NAKAE and K. OKADA

Department of Materials Science and Engineering, School of Science and Engineering, Waseda University, Tokyo 169, Japan

(Received 26 January 1993)

Abstract—An improved sessile drop technique which prevented the oxidation of aluminum was used to measure the changes in contact angle between boron nitride and molten aluminum in a purified He–3% H_2 between 1173 and 1373 K. The contact angle progressed through the four wetting phases similar to other ceramics when the results were plotted on a logarithmic time scale. However, at and above 1273 K the equilibrium contact angle was 0° which is much less than those of typical ceramics. Using the value in phase II, the original contact angle between boron nitride and aluminum (contact angle between non-reacted boron nitride and aluminum) was estimated to be 133° at 1373 K. The wetting progressed by producing another non-wetting material, AlN, in this non-wetting system. The detailed mechanism of the solid/liquid/vapor interfacial advance during wetting in such a system was also explained using Cassie's equation.

Résumé—Une technique améliorée de la goutte posée évitant l'oxydation de l'aluminium a été employée pour mesurer les variations de l'angle de contact entre du nitrure de bore et de l'aluminium en fusion sous une atmosphère purifiée d'He–3% H_2, entre 1173 et 1373 K. L'angle de contract évolue à travers les quatre phases de mouillage comparables à celles des autre céramiques lorsqu'on reporte les résultats sur un diagramme à échelle logarithmique. Cependant, à et au-dessus de 1273 K, l'angle de contact d'équillibre était égal à 0 degré, c'est à dire très inférieur à celui de céramiques typiques. En utilisant la valeur en phase II, l'angle de contact original entre le nitrure de bore et l'aluminium (angle de contact entre le nitrure de bore non-transformé et l'aluminium) a été estimé à 133° à 1373 K. Dans ce système non-mouillable, la mouillabilité évolue en produisant un autre matériau non-mouillant AlN. Le mécanisme détaillé de la progression de l'interface solide/liquide/gaz durant le processus de mouillage dans un tel système a également été expliqué en utilisant l'équation de Cassie.

Zusammenfassung—Zum Messen der Änderungen im Kontaktwinkel zwischen Boronnitrid und geschmolzenem Aluminium in verfeinertem He–3% H_2 zwischen 1173 und 1373 K wurde eine verbesserte statische Tropfmethode verwendet, welche die Oxydation des Aluminiums verhütet. Der Kontaktwinkel ändert sich ähnlich wie bei anderen Keramikmaterialien über die vier Benetzungsphasen hinweg, wenn die Ergebnisse mit einer logarithmischen Zeitskala aufgezeichnet werden. Ab 1273 K wird der Gleichgewichtskontaktwinkel jedoch zu 0 Grad und damit viel kleiner als für typische Keramikmaterialien. Unter Verwendung des Wertes in Phase II wird der Originalkontaktwinkel zwischen Boronnitrid und Aluminium (der Kontaktwinkel zwischen nichtreagiertem Boronnitrid und Aluminium) bei 1373 K auf 133° geschätzt. Die Benetzung schritt durch Erzeugung eines anderen, nicht benetzenden Materials, AlN, in dieses nichtbenetzende System fort. Der detaillierte Mechanismus des Fortschritts der Fest-/Flüssig/Gasgrenzfläche während der Benetzung in einem solchen System wird auch durch Verwendung der Cassie-Gleichung erklärt.

1. INTRODUCTION

The wetting of ceramic surfaces by molten metals is one of the most important phenomena to consider when designing a metal matrix composite material. The addition of ceramic particles into a molten metal has the benefit of enabling us to manufacture an almost perfectly shaped composite material easily. However, the success of this method depends on the wetting, which is usually problematic. As the contact angle between the ceramic particles and the molten metal decreases, the external force required for inserting particles into a melt becomes smaller. When the contact angle is 0°, particles can be inserted into a melt without external forces. However, the contact angles for typical ceramics are usually greater than 90°.

The wetting of ceramics by molten metals usually involves interfacial reaction wetting [1, 2] (wetting accompanied by the interfacial reactions). The interfacial reactions produce new compounds at the interface and change the composition of the liquid metals and ceramics. As a result, all of the solid/liquid, liquid/vapor and solid/vapor interfacial free energies change [3].

The decrease in the contact angle of aluminum on boron nitride was considerably larger than the decrease associated with typical ceramics. The unique relationship between the wetting and the interfacial reactions is also important. Therefore, the driving

Table 1. Calculated oxygen partial pressure in equilibrium using the equation:

$$4Al(l) + 3O_2(g) = 2Al_2O_3(s)$$

Temperature (K)	P_{O_2} (Pa)
1073	4.260×10^{-39}
1173	2.048×10^{-34}
1273	1.810×10^{-30}
1373	4.257×10^{-27}

force and the mechanism of the interfacial-reaction wetting are discussed in this paper.

2. OXIDATION OF ALUMINUM

It is well known that aluminum is easily oxidized. Once an aluminum oxide film is formed on the aluminum surface the oxide film seems to prevent the interface from advancing and the contact angle from decreasing. In order to measure the contact angle correctly, atmospheric conditions under which aluminum does not oxidize must be achieved.

$$4Al(l) + 3O_2(g) = 2Al_2O_3(s) \quad (1)$$

$$\Delta G^\circ = -3384270 + 662.88T \quad [4]. \quad (2)$$

When it is assumed that the activity of aluminum and the activity of Al_2O_3 are one due to the fact that the solubility of oxygen in aluminum is very slight, the oxygen partial pressure in equilibrium (P_{O_2}) is calculated as shown in Table 1.

Since the oxygen partial pressure, as shown in Table 1, cannot actually be obtained it seems that the oxidation of aluminum cannot be prevented. However, at higher temperatures the production of a gas (Al_2O) becomes more important than at low temperatures [5], as shown in the following equation

$$4Al(l) + O_2(g) = 2Al_2O(g) \quad (3)$$

$$\Delta G^\circ = -341410 - 98.74T \quad [4]. \quad (4)$$

Therefore, the following equation is obtained from equations (1)–(4)

$$Al_2O_3(s) = Al_2O(g) + O_2(g) \quad (5)$$

$$\Delta G^\circ = 1521430 - 380.81T. \quad (6)$$

Assuming that the partial pressures of Al_2O and O_2 are equal, the equilibrium pressure becomes as shown in Table 2. Although the oxygen partial pressures in equation (5) are much higher than those in equation (1), they are also not actually obtainable.

Furthermore, the reaction between Al and Al_2O_3 which produces Al_2O is considered as the following equation [5]

$$4Al(l) + Al_2O_3(s) = 3Al_2O(g) \quad (7)$$

$$\Delta G^\circ = 1180020 - 479.55T. \quad (8)$$

Using these equations, the equilibrium Al_2O partial pressure is calculated as shown in Table 3. The oxygen partial pressures shown in Table 3 are very high. However, since the aluminum is usually covered by an oxide film, Al_2O cannot be easily removed. Therefore, the reaction shown in equation (7) cannot actually occur according to the chemical kinetics. However, when a part of the oxide film is removed, Al_2O can vaporize easily, and the Al_2O_3 starts to deoxidize. Accordingly, it is most important that the original oxide film is effectively removed, after this operation the correct contact angles can be accurately measured.

3. EXPERIMENTAL PROCEDURE AND APPARATUS

3.1. Improved sessile drop method apparatus

The sessile drop method has been widely used to estimate the wetting of various materials. In ceramic/metal systems the metal is usually placed on the ceramic surface in a solid state before heating. Then, the sample is heated to melt the metal on the ceramic surface. When this normal sessile drop method is applied to the measurement of wetting by aluminum, the oxidation of aluminum cannot be prevented since the initial oxide film is not removed, as discussed in Section 2. Furthermore, while the sample is being heated, the ceramic sample reacts with the metal, therefore the original contact angle cannot be measured.

In order to achieve the following objectives, an improved sessile drop method [1] was devised.

(1) Initial surface oxide film is removed.
(2) The time at which the wetting starts is decided.
(3) Contamination of the ceramic surface by evaporated aluminum is minimized.
(4) An advancing contact angle in phase I and phase II [1, 2] (Initial phases: see Section 4) can be produced.
(5) The condition under which aluminum does not oxidize throughout the wetting experiments is achieved.

A schematic diagram of the improved sessile drop method apparatus is shown in Fig. 1. The system

Table 2. Calculated oxygen and Al_2O partial pressure in equilibrium using the equation:

$$Al_2O_3(s) = Al_2O(g) + O_2(g)$$

Temperature (K)	P_{Al_2O} ($=P_{O_2}$) (Pa)
1073	8.283×10^{-23}
1173	1.190×10^{-19}
1273	5.451×10^{-17}
1373	1.023×10^{-14}

Table 3. Calculated Al_2O partial pressure in equilibrium using the equation:

$$4Al(l) + Al_2O_3(s) = 3Al_2O(g)$$

Temperature (K)	P_{Al_2O} (Pa)
1073	6.419×10^{-6}
1173	6.908×10^{-5}
1273	1.641×10^{-3}
1373	2.460×10^{-2}

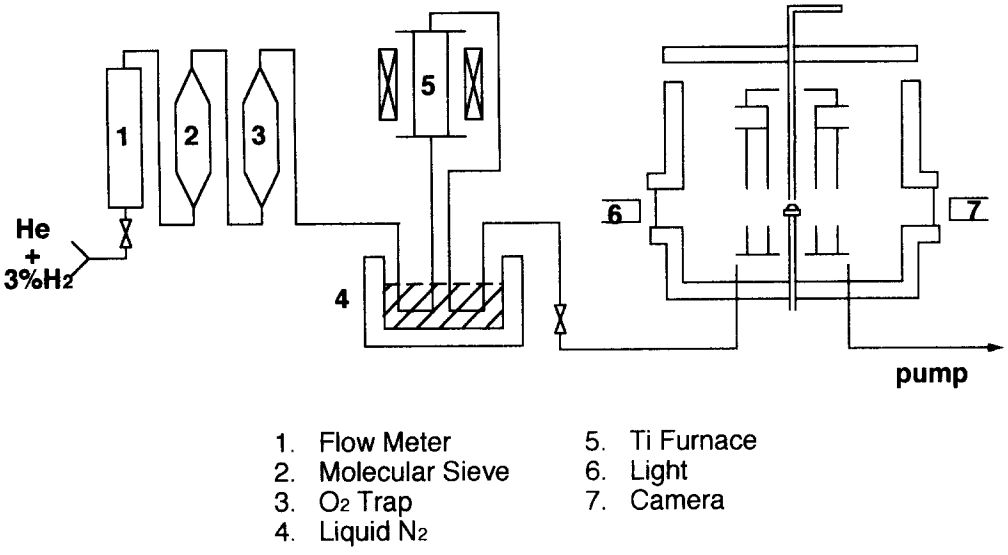

Fig. 1. Improved sessile drop method apparatus.

consists of a sealed chamber, a purification system for the atmospheric gas (He–3% H_2) in the chamber, a set of vacuum pumps to evacuate the chamber, two light sources, and two cameras: a 35 mm camera and a video recording camera both with bellows and macro lenses.

The sealed chamber has four windows and contains a molten aluminum dropping device and a molybdenum cylindrical heater with three concentric reflectors located around the dropping device.

As shown in Fig. 2, the aluminum dropping device is a tube of pure alumina (99.9 mass %) with a 0.5 mm hole at its base. When the temperature of the substrate reaches the experimental temperature, an aluminum pellet placed outside the furnace is pushed along the tube by a steel rod using a magnet and dropped into the bottom of the dropping tube. Immediately after the aluminum pellet has been heated to the experimental temperature, it is, as a liquid, slowly forced through the hole at the base of the tube by a very gradual decrease in the atmospheric pressure of the chamber.

At this time, the initial oxide film is removed mechanically by the action of passing through the hole and initial wetting begins. Furthermore, the contamination of the ceramic surface by evaporated aluminum is minimized because the aluminum is in a molten state for only a very short period of time. The rate of dropping is thus minimized and the gas flow due to the difference in pressure between the chamber and the tube stops as soon as the drop passes through the hole. The slow drop rate maximizes the possibility of obtaining an advancing or equilibrium contact angle instead of a receding one.

The gas purification system [1] consists of a molecular sieve for trapping H_2O, an oxygen trap, liquid nitrogen cold trap and sponge titanium furnace heated to about 1173 K to remove H_2O and O_2 from the atmospheric gas so that oxidation of the aluminum surface is prevented during each experiment. One liquid nitrogen cold trap was placed before the titanium furnace and the other was placed after it in order to trap the titanium vapor as well as any extra H_2O.

The wetting was not measured in a vacuum because under such a condition the loss of aluminum due to vaporization is so great that the contact angle becomes a receding contact angle and therefore affects the validity of the experimental results [1]. When the wetting by aluminum is measured in an atmosphere, the partial pressure of oxygen must be low enough for Al_2O to move relatively quickly onto the chamber wall (where the temperature is low). The movement

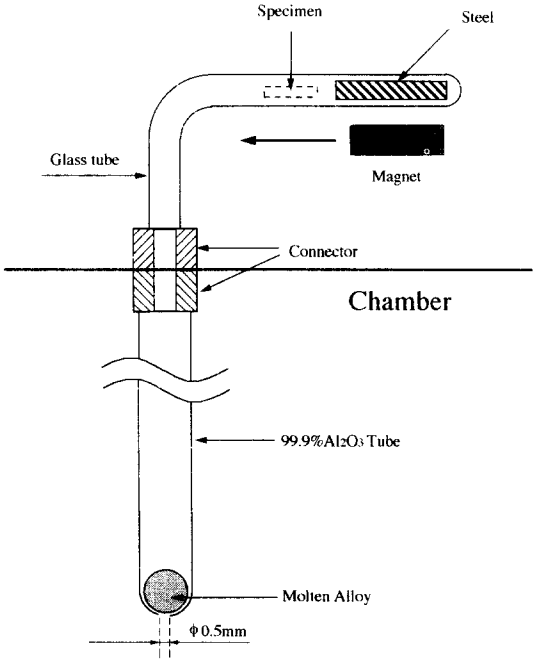

Fig. 2. Schematic of dropping device.

Table 4. Chemical composition of h-BN (mass %)

BN	B_2O_3	CaO	Al	Fe	Mg	C
>99.7	0.06	0.005	<0.001	<0.001	<0.001	0.04

of O_2 onto the aluminum surface must be slow enough, as compared to the movement of Al_2O, to prevent oxidation of the aluminum. Therefore, an atmosphere which contains very few oxygen molecules is the best condition for measuring the wetting by aluminum. We believe such an atmosphere is attained in this apparatus.

3.2. Experimental procedure

The experiments were conducted using 99.99% Al pellets and plates of 99.7% sintered h-BN manufactured by Shin-Etsu Chemical Co. The Al pellets weighed about 70 mg each and were pre-treated by immersion in hydrofluoric acid and then in acetone. Since only a few impurities in ceramics can affect the wetting [6, 7], the highest possible purity ceramics available at present were used. Table 4 gives the chemical composition of BN. The plates had dimensions of $20 \times 20 \times 5$ mm. The BN plates were polished to a mirror finish using various grades of SiC paper and two grades of diamond paste (particle diameter 6 and 0.25 μm) before being cleaned in acetone within an ultrasonic cleaner.

After the BN plate was set in a horizontal position under the dropping device, the chamber was evacuated to 1.3×10^{-3} Pa (approx. 10^{-5} torr) and heated at 1423 K. This temperature was maintained for about 3600 s to remove hydroxyl groups mainly before the purified He–3% H_2 atmospheric gas was introduced and the pressure raised to 120 kPa (1.2 atm). The chamber was then cooled and when the BN plate reached the requisite experimental temperature (1173, 1273 and 1373 K), the Al pellet was inserted into the dropping device. Immediately after the Al pellet was raised to the experimental temperature it was, as a liquid, forced through the hole in the base of the tube. At this time, if the oxide film could not be removed, the results of the drop cycle were disregarded and the experiment was repeated.

When a receding contact angle results from the drop, that is, when the interfacial area is larger than the equilibrium area, it is difficult for the contact angle to reach equilibrium. One of the reasons for this difficulty is that the center of gravity of the sessile drop is rising. If the interfacial diameter decreases to the equilibrium diameter, the γ_{sv} of the ceramic surface that was in contact with the molten aluminum will be decreased due to its contamination from contact with the aluminum. Furthermore, when the new products are formed at the solid/liquid interface, the surface is rougher and the difference between a receding contact angle and the equilibrium contact angle is larger. Therefore, only advancing or equilibrium contact angles are suitable for measuring wetting.

The improved sessile drop method allowed us to obtain a greater percentage of advancing or equilibrium contact angles. When a receding contact angle resulted in phase I or II [1, 2] (initial phases: see Section 4), the value was disregarded and the experiment repeated.

The sessile drop was photographed with a 35 mm camera at 5 and 10 s and then at 10 s intervals for the first 60 s, and thereafter at intervals of 60, 180, 360 and 600 s until the end of the drop cycle (7.2 ks). Right and left hand contact angle θ were measured on projections of the monochrome negatives (magnification 50 ×). When θ was larger than 100°, the value was calculated using Bashforth and Adam's tables [8]. When θ was less than 100°, the contact angles were measured directly because the contact angle obtained using Bashforth and Adam's tables had a large margin of error. If the contact angles recorded by the two cameras differed by more than a few degrees, or if the bulk drop was unsymmetrical then the results of the drop cycle were disregarded and the experiment was repeated.

In order to observe the interfacial advancing phenomena in detail, a video camera was used with a filter devised to remove the radiant light from the heater.

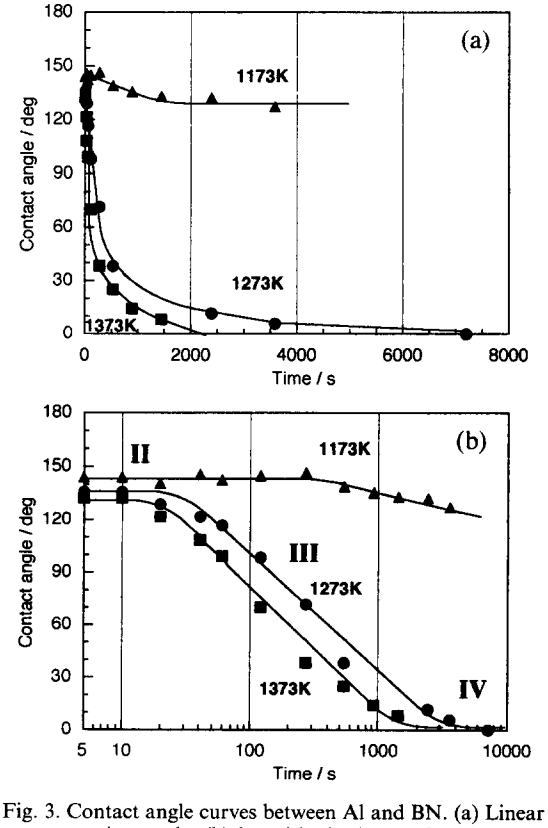

Fig. 3. Contact angle curves between Al and BN. (a) Linear time scale; (b) logarithmic time scale.

Table 5. Comparison on contact angle between boron nitride and aluminum

Researcher	Atmosphere	1273 K	1373 K
Naidich [9]	Unknown	—	<90°
Nicholas [10]	Vacuum	90°	35°
Chiaramonte [11]	Vacuum	50°	—
Xue [12]	Vacuum	72°[a]	34°[b]
This work	He–3% H_2	0°	0
This work	Vacuum	0°	0

[a]1280 K, [b]1380 K

4. EXPERIMENTAL RESULTS

Figure 3 shows the contact angle curves for each of the three experimental temperatures, as plotted on a normal (linear) and a logarithmic time scale. When the contact angle curves were plotted on a logarithmic time scale, as shown in Fig. 3(b), the contact angles can be seen to progress through the four phases [1, 2] similar to other ceramics, viz: I—original wetting phase (0–5 s); II—quasi-equilibrium phase; III—interfacial-reaction-wetting phase; IV—equilibrium phase.

An aluminum drop vibrates for a few seconds after contacting the ceramic plate with the contact angle decreasing from an initial 180°. Since the contact angles have large margins of error in phase I, because of the vibration of the aluminum drop, this phase is not shown in Fig. 3.

In phase II the original contact angle (the contact angle between non-reacted BN and aluminum) can be determined [1, 2]. The original contact angle is about 143°, 135° and 132° at 1173, 1273 and 1373 K respectively.

Phase III was observed at and above 1173 K, while phase IV was observed at and above 1273 K. The equilibrium contact angle (phase IV) is 0°. This value is much lower than those of typical ceramics. This value means that BN is an optimum material for use as an aluminum matrix composite material from the standpoint of wetting.

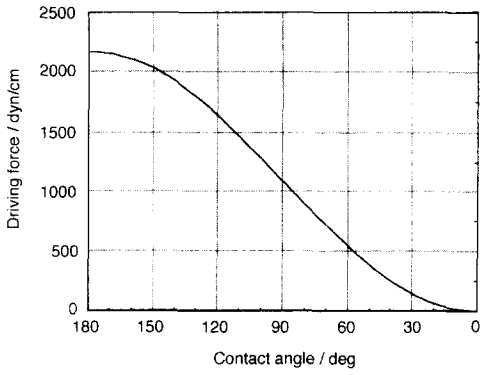

Fig. 4. Relationship between contact angle and driving force of wetting.

5. DISCUSSIONS

5.1. Comparison with other researchers' values

Table 5 shows the contact angles between boron nitride and aluminum reported by other researchers [9–12]. The values shown in this table are very different from each other, and the value 0° observed in this study is much smaller than the values of the other studies. However, Meaders *et al.* reported that the melting aluminum climbed the boron nitride wall [13]. This phenomenon indicated that the contact angle was 0° during their experiments.

In a system whose equilibrium contact angle is θ_e, the balance of the three interfacial tensions is $\gamma_{SV} - \gamma_{SL} = \gamma_{LV} \cos \theta_e$ as derived from Young's equation. When the contact angle is θ in this system, the driving force of wetting (F) which causes the system to reach equilibrium is expressed as equation (9)

$$F = \gamma_{SV} - \gamma_{SL} - \gamma_{LV} \cos \theta$$
$$= \gamma_{LV}(\cos \theta_e - \cos \theta). \quad (9)$$

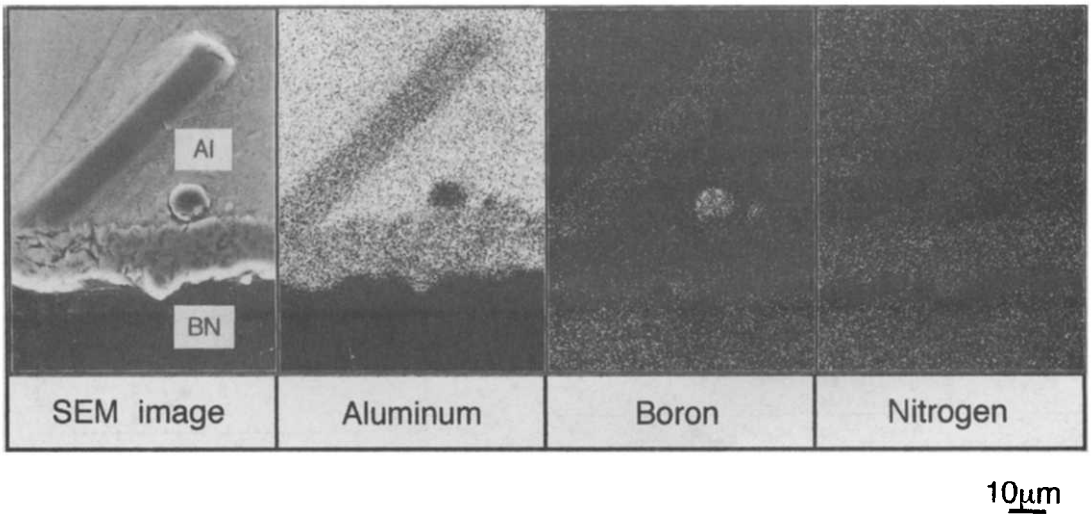

Fig. 5. X-ray mappings of BN/Al interface (1373 K, 7200 s).

When the contact angle is θ in a system whose equilibrium contact angle is 0°, the driving force of wetting (F) is expressed in equation (10)

$$F = \gamma_{LV}(1 - \cos\theta). \quad (10)$$

As the contact angle becomes smaller, the driving force of wetting also decreases as shown in Fig. 4. Therefore, if there is a limiting factor, such as an oxide film on the aluminum surface, the drop will stop spreading, resulting in a halt in the decrease of the contact angle. Accordingly, the value of the final contact angle probably depends on the extent of the limiting factors, such as, the quantity of oxide film on the aluminum surface.

In this experiment the aluminum oxide film was removed by passing the aluminum drop through the 0.5 mm ϕ aperture of a Al_2O_3 tube. Furthermore, the partial pressure of oxygen was extremely low because the He–3% H_2 gas was purified by passing it through liquid nitrogen and a titanium furnace, this also prevented oxidation during the experiment. In ordinary sessile drop experiments, the aluminum is placed on the substrate before it is heated, therefore the initial oxide film on the aluminum surface is not completely removed, even when the experiment is conducted in an ultra high vacuum. We believe that because of this factor the contact angle observed by other researchers was larger than that obtained in the present study.

5.2. *Solid/liquid interface reaction*

Figure 5 shows a secondary electron image and X-ray mappings of a cross section of a 1373 K drop cycle sample. With EPMA line analyses of the typical cross-section aluminum and nitrogen were detected within the reaction zone while boron was not. Boron was only detected in the aluminum. Using an X-ray diffractometer, the structure of the reaction zone was found to be AlN. Therefore, the initial reaction equation at the interface is as follows

$$BN(s) + Al(l) \rightarrow AlN(s) + B(\text{in Al}). \quad (11)$$

Since the volume of AlN produced is about 5.6 mm^3 at 1373 K as shown in Table 6, it is estimated that the aluminum must contains 6.2 mass % boron.

At 1373 K boron dissolves into aluminum to make up about 3% of the mass of the aluminum, as shown in the Al–B binary phase diagram [14]. Above 1258 K the remaining boron becomes αAlB_{12}, whereas it becomes AlB_2 below 1258 K. The chemical equations during the experiments are as follows

Table 6. Volume of the produced AlN

Temperature (K)	Depth of reaction zone (μm)	Volume of produced AlN (mm^3)
1173	15	0.12
1273	14	5.2
1373	7	5.6

$$BN(s) + Al(l) \rightarrow AlN(s) + B(\text{in Al}) + \alpha AlB_{12}(s) \quad (>1258\ K) \quad (12)$$

$$BN(s) + Al(l) \rightarrow AlN(s) + B(\text{in Al}) + AlB_2(s) \quad (<1258\ K). \quad (13)$$

Two kinds of boron compounds were detected in the aluminum of a 1373 K drop cycle as shown in Fig. 5, a rectangular shaped compound and a round shaped compound. αAlB_{12} must have been produced at 1373 K during the experiments. Also, AlB_2 can be produced in the sample during cooling after the experiments. It is considered that the round shape, which has a stronger peak of boron, is αAlB_{12} and the rectangular one, which has a weaker peak of boron, is AlB_2.

αAlB_{12} and AlB_2 were not detected uniformly throughout the interface. Therefore, these compounds did not affect the wetting very much. Furthermore, since boron is not a surfactant of aluminum, according to the results reported by Lang [15], it does not affect the solid/liquid interfacial tension so much, either.

5.3. *Driving force for contact angle decrease*

The original contact angle between the boron nitride and the aluminum (phase II) is about 132° and we know that B, αAlB_{12} and AlB_2 do not affect the wetting very much, as mentioned above. Therefore, it is considered that the production of AlN at the interface causes the contact angle to decrease to 0°.

Figure 6 shows the contact angle between aluminum nitride and aluminum [7] compared with the contact angle between boron nitride and aluminum at 1373 K. This figure shows that aluminum nitride is also a non-wetting material. Therefore, in this system the production of a new non-wetting compound in the non-wetting material causes the contact angle to decrease.

In order to explain this characteristic phenomenon a model was formulated, as shown in Fig. 7. The contact angle is determined not by the absolute value of each of the interfacial tensions, but by the difference between the solid/liquid interfacial tension (γ_{SL})

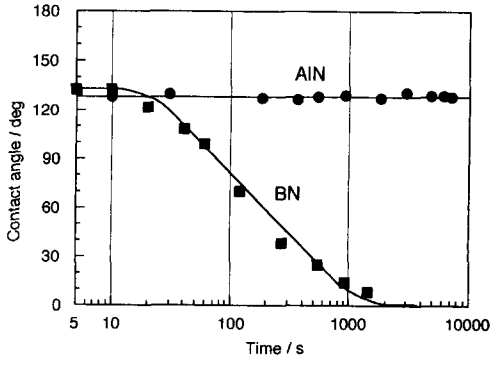

Fig. 6. Contact angle curves of AlN/Al and BN/Al at 1373 K.

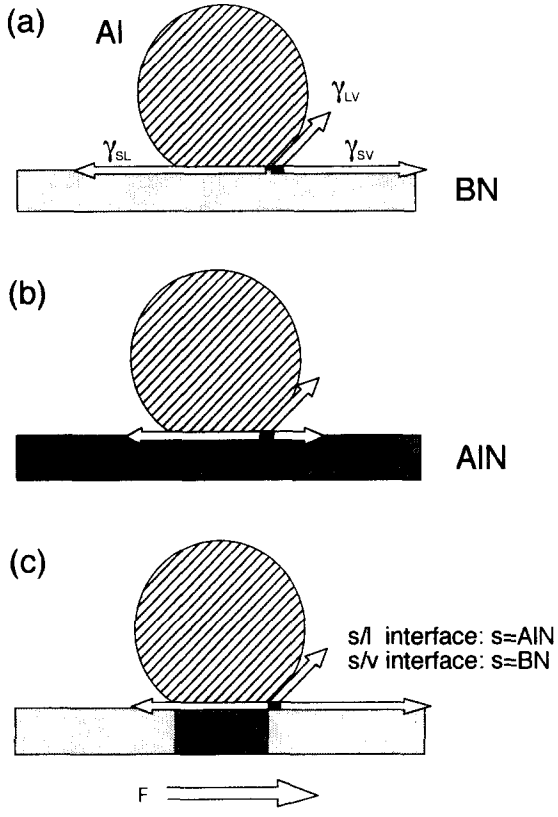

Fig. 7. Driving forces of wetting of BN/Al system.

and the solid/vapor interfacial tension (γ_{SV}). Also the contact angle (θ) is determined by the following equation

$$\cos\theta = \frac{\gamma_{SV} - \gamma_{SL}}{\gamma_{LV}} \tag{14}$$

where γ_{LV} is liquid/vapor interfacial tension. Therefore, even when the contact angle is the same in several systems, there are many conditions to be considered. When the metal is the same (Al in this case), that is, when γ_{LV} is the same, the difference ($\gamma_{SV} - \gamma_{SL}$) is the only factor that determines the contact angle.

The difference ($\gamma_{SV} - \gamma_{SL}$) is similar in BN/Al and AlN/Al systems, since the original contact angles of both systems are similar. Accordingly, when it is assumed that in the BN/Al system both γ_{SV} and γ_{SL} are large and in the AlN/Al system both interfacial energies are small, the decrease in the contact angle to 0° can be clearly explained as shown in Fig. 7(c). When AlN is produced only at the solid/liquid interface, γ_{SV} (namely $\gamma_{BN\text{-}V}$) is large and γ_{SL} (namely $\gamma_{AlN\text{-}L}$) is small and as a result there is a driving force for the contact angle to decrease.

Figure 8 shows the interface of a sample cooled quickly 2 min after the Al drop. This figure shows that AlN is produced only at the solid/liquid interface. This phenomenon does not contradict the model shown in Fig. 7. However, the estimation of the balance between the solid surface tension and the

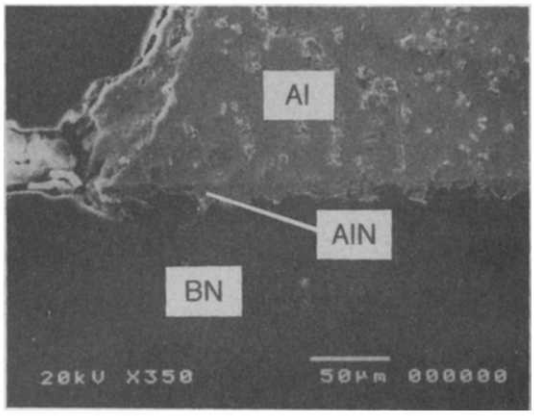

Fig. 8. Appearance of BN/Al interface (1373 K, 720 s).

solid/liquid interfacial tension, as shown in Fig. 7, cannot be confirmed since both values cannot be easily measured and few values have been reported. Contrariwise, a calculated surface tension value of h-BN (100) was reported by Xue [12] and the critical surface tension of AlN was reported by Rhee [16]. The calculated surface tension of h-BN (100), which should have the lowest surface tension of all h-BN surfaces, is 1030 mN/m, whereas the critical surface tension of AlN is 664 mN/m. According to Rhee [17], the critical surface tension is equal to the surface tension of AlN (γ_{SV}). Although both values include some assumptions, these values affirm the estimations of Fig. 7.

When the molten aluminum is in a condition corresponding to (a) in Fig. 9, the stable contact angle is about 0°. When the aluminum advances to reach the condition corresponding to (b), the stable contact angle is 132°, since the solid of solid/liquid interface

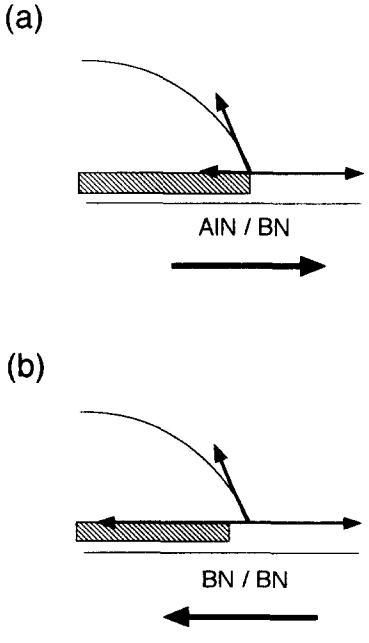

Fig. 9. Two types of solid/liquid/vapor interface.

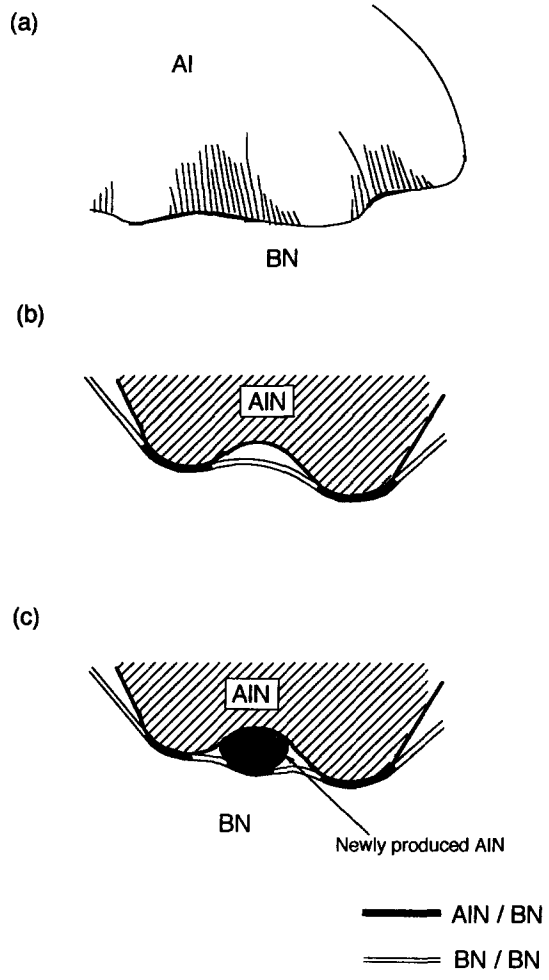

Fig. 10. A model of interface advancing.

also becomes BN. In phase III, the contact angle is decreasing in a range between 0° and 132° and is different from the two stable contact angles. Therefore, the state of the solid/liquid/vapor interface in this phase must be a combination of AlN/BN [condition (a)] and BN/BN [condition (b)], as shown in Fig. 10. Seen from the top, the solid/liquid/vapor interface is as shown in Fig. 10(a). If the interface is represented without the aluminum it should appear as shown in Fig. 10(b). It is considered, as shown in Fig. 10(b), that the AlN/BN interface, which has a stable contact angle of 0°, pulls the solid/liquid/vapor interface forward, thereby producing BN/BN interface, which has a stable contact angle of 132°. When new AlN is produced, as shown in Fig. 10(c), the solid/liquid/vapor interface also advances and changes the shape of the solid/liquid/vapor interface. Accordingly, the interface advances with a laterally waving motion.

The advancing lateral movement of the leading edge of the solid/liquid/vapor interface was observed with a video camera as shown in Fig. 11. These photos indicate that the model proposed here is suitable for the representation of the phenomenon.

The ratio of AlN/BN and BN/BN at the solid/liquid/vapor interface depends on the condition of the AlN produced. However, the ratio of AlN/BN at the solid/liquid/vapor interface can be roughly estimated using Cassie's equation [18], but only for the solid/liquid/vapor interface. Since the contact angle at any given time, is determined by the balance at the interfacial forces, Cassie's equation essentially should be applied only to the solid/liquid/vapor interface, as follows

$$\cos\theta_t = x\cos\theta_{AlN/BN} + (1-x)\cos\theta_{BN/BN}$$
$$= x\cos 0^\circ + (1-x)\cos 132^\circ \qquad (15)$$

where $\cos\theta_t$ is the cosine of the contact angle at an arbitrary time t and x is the ratio of AlN/BN at the solid/liquid/vapor interface. Using equation (15), the change in the ratio of AlN/BN and BN/BN over time is calculated as shown in Fig. 12. This figure shows that the ratio of AlN/BN increases as the solid/liquid/vapor interface advances.

6. SUMMARY

In order to measure the change in the contact angle between hexagonal boron nitride (h-BN) and aluminum over time, an improved sessile drop technique was devised to prevent the oxidation of aluminum.

1. It was confirmed that above a certain temperature the contact angle of Al on BN also progresses through the following four phases, similar to other

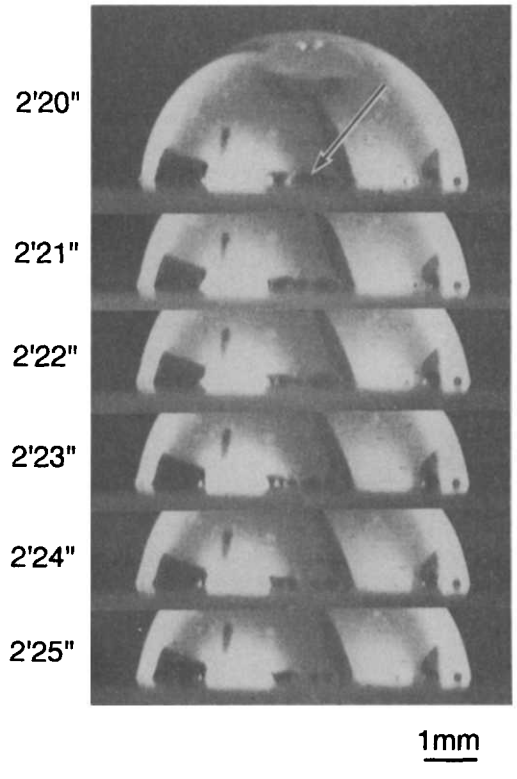

Fig. 11. Interface advance with laterally waving motion.

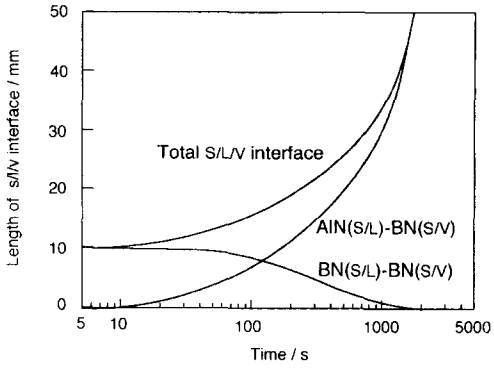

Fig. 12. Change in length of solid/liquid/vapor interface over time.

ceramics, on a logarithmic time scale: I—original wetting phase; II—quasi-equilibrium phase; III—interfacial-reaction-wetting phase, IV—equilibrium phase.

2. The original contact angle between boron nitride and aluminum was about 143°, 135° and 132° at 1173, 1273 and 1373 K respectively.

3. At temperatures higher than 1273 K, the equilibrium contact angle between BN and Al becomes 0°. This contact angle indicates that BN is an appropriate material for inserting into liquid Al.

4. The degree of decrease in the contact angle depends on the initial quantity of oxide film on the aluminum. Thermodynamics considerations have indicated that the conditions for the reduction are easily achieved when the initial oxide film on aluminum surface is partially removed. When the oxidation of the aluminum is prevented, the contact angle becomes 0°.

5. The production of aluminum nitride, which is a non-wetting material, decreases the contact angle. Only the production of aluminum nitride at the solid/liquid interface can produce a driving force for decreasing the contact angle.

6. Essentially, Cassie's equation should only be applied to the solid/liquid/vapor interface because an increase or decrease in the total free energy is determined by the movement of the solid/liquid/vapor interface. Only in the case where new products are dispersed uniformly can Cassie's equation be applied to the whole solid/liquid interface, as Cassie suggested.

Acknowledgement—This study was carried out with the support of the Light Metal Educational Foundation Inc. The authors wish to express their appreciation for this support.

REFERENCES

1. N. Yoshimi, H. Nakae and H. Fujii, *Mater. Trans. Japan Inst. Metals* **31,** 141 (1990).
2. H. Nakae, H. Fujii and K. Sato, *Mater. Trans. Japan Inst. Metals* **33,** 400 (1992).
3. I. A. Aksay, C. E. Hoge and J. A. Pask, *J. Phys. Chem.* **78,** 1178 (1974).
4. Hitetsu Kinzoku Seiren, *Japan Inst. Metals*, p. 315 (1980).
5. V. Laurent, D. Chatain, C. Chatillon and N. Eustathopoulos, *Acta metall.* **36,** 1797 (1988).
6. H. Fujii and H. Nakae, *ISIJ Int.* **30,** 1114 (1990).
7. H. Fujii, H. Nakae and K. Okada, *Metall. Trans.* **24A,** 1391 (1993).
8. F. Bashforth and J. C. Adams, *An Attempt to Test the Theories of Capillary Action*, p. 82. Cambridge Univ. Press, London (1883).
9. Y. Naidich, *Prog. Surf. Membr. Sci.* **14,** 353 (1981).
10. M. G. Nicholas, D. A. Mortimer, L. M. Jones and R. M. Crispin, *J. Mater. Sci.* **25,** 2679 (1990).
11. F. P. Chiaramonte and B. N. Rosenthal, *J. Am. Ceram.* **74,** 658 (1991).
12. X. M. Xue, J. T. Wang and M. X. Quan, *J. Mater. Sci. Engng A* **132,** 277 (1991).
13. J. C. Meaders and M. D. Carithers, *Rev. Sci. Inst.* **37,** 612 (1955).
14. T. B. Massalski *et al.*, *Binary Alloy Phase Diagrams*, Vol. 1, p. 91. Am. Soc. Metals, Metals Park, Ohio (1986).
15. G. Lang, *ALUMINUM* **50,** 731 (1974).
16. S. K. Rhee, *J. Am. Ceram. Soc.* **53,** 386 (1970).
17. S. K. Rhee, *J. Am. Ceram. Soc.* **53,** 639 (1970).
18. A. B. D. Cassie, *Discussions Faraday Soc.* **3,** 11 (1948).